

Angle-adjustable density field formulation for the modeling of crystalline microstructureZi-Le Wang,¹ Zhirong Liu,^{1,*} and Zhi-Feng Huang^{2,†}¹*College of Chemistry and Molecular Engineering, Peking University, Beijing 100871, China*²*Department of Physics and Astronomy, Wayne State University, Detroit, Michigan 48201, USA*

(Received 25 January 2018; published 25 May 2018)

A continuum density field formulation with particle-scale resolution is constructed to simultaneously incorporate the orientation dependence of interparticle interactions and the rotational invariance of the system, a fundamental but challenging issue in modeling the structure and dynamics of a broad range of material systems across variable scales. This generalized phase field crystal-type approach is based upon the complete expansion of particle direct correlation functions and the concept of isotropic tensors. Through applications to the modeling of various two- and three-dimensional crystalline structures, our study demonstrates the capability of bond-angle control in this continuum field theory and its effects on the emergence of ordered phases, and provides a systematic way of performing tunable angle analyses for crystalline microstructures.

DOI: [10.1103/PhysRevB.97.180102](https://doi.org/10.1103/PhysRevB.97.180102)

One of the long-lasting challenges in materials study is how to effectively tackle the complex structural and dynamical phenomena involving multiple spatial and temporal scales. Of particular importance is the bridging between atomic-level microstructural details and mesoscopic, nonequilibrium characteristics, such as mesoscale surface patterns or interface structures that are governed by system elasticity and plasticity and by diffusional or displacive dynamic processes. This requires novel theoretical efforts, particularly those based on coarse-graining methods beyond the traditional single-scale atomistic or continuum approaches. Among them much work has been devoted to the development of density-field-based schemes across different scales, as featured by the incorporation of crystalline and microscopic attributes into the probability density description [1–4].

Many of these field-based models can be connected to the classical density functional theory (CDFT) [5,6]. Through coarse graining or “smoothing” the local density field over atomic vibrational scales, the small-scale limitation of CDFT can be mitigated, resulting in a continuum field theory with an atomic- or particle-scale spatial resolution and diffusive timescales. A fast-growing and widely applied version of such a theory is the phase field crystal (PFC) method [1,2,7–14], with applications across a variety of solid and soft-matter systems, particularly for the elastoplastic phenomena that are inaccessible using traditional methods [15–23]. Most PFC models are constructed for systems of isotropic interactions, with the lattice symmetry controlled by microscopic length scales [1,2,7–14,24–26]. They are applicable to metallic-type materials or colloidal systems with excluded volume or steric interactions that are dependent on interparticle distance, but would be a crude approximation if applied to a broader range

of material systems with directional interactions depending on both bond lengths and angles. It is thus important to build the bond (or particle-neighboring) angle dependency into continuum modeling which, however, is nontrivial, given that microscopically the corresponding interparticle interactions are *anisotropic*, while *rotational invariance* of the whole system must be maintained in the free-energy functional.

In the traditional density-field approach based on Landau theory, an additional bond-orientational order parameter and the associated rotationally invariant orientational free energy were introduced for glassy [27] or quasicrystalline [28] systems. On the other hand, in principle, the orientational information should already be incorporated in the density functional and direct correlation functions, although it is challenging to identify and control. The related attempts are rather limited, and are usually accompanied by some specific assumptions, as in two types of angle-dependent PFC models developed recently. The first one [29] adopts some nonlinear free-energy gradient terms introduced in previous studies of the square convection pattern [30,31], while the second type is built on some preassumed infinite series expansions of the three-point direct correlation function $C^{(3)}$, either through a separation of $C^{(3)}$ in real space [32] or in terms of Legendre polynomials in Fourier space [33].

Here, we provide a systematic study of angular dependence and orientation control in a density field formulation. Our analysis is based on the property of the isotropic tensor and the complete Fourier expansion of any n -point direct correlation function $C^{(n)}$ that satisfies the condition of rotational invariance, without any preassumptions. Our results show that any finite-order contributions of $C^{(3)}$ expansion to the rotationally invariant free energy are always angle independent, as a result of the resonant condition of the wave-vector triads, while those from at least a four-point correlation are needed to explicitly incorporate the dependency on the angle between neighboring constituent particles. Applications of this PFC-type model

*liuzhirong@pku.edu.cn

†huang@wayne.edu

include some examples of three-dimensional (3D) structure modeling (such as simple cubic and diamond cubic phases) via a single length scale combined with angle-dependent effects, and, importantly, the achievement of continuous angle control in both two-dimensional (2D) and 3D crystalline structures such as 2D rhombic and square and 3D simple monoclinic and orthorhombic phases, which demonstrates the advantage of this angle-adjustable density field approach.

In CDFT the free-energy functional is expanded via direct correlation functions [5,6], i.e.,

$$\begin{aligned} \Delta F/k_B T &= \rho_0 \int d\mathbf{r} (1+n) \ln(1+n) - \sum_m \frac{1}{m!} \rho_0^m \\ &\times \int \prod_{j=1}^m d\mathbf{r}_j C^{(m)}(\mathbf{r}_1, \mathbf{r}_2, \dots, \mathbf{r}_m) \\ &\times n(\mathbf{r}_1) n(\mathbf{r}_2) \cdots n(\mathbf{r}_m), \end{aligned} \quad (1)$$

where $n = (\rho - \rho_0)/\rho_0$ is the density variation field, with ρ the local atomic number density and ρ_0 a reference state density. The condition of rotational invariance needs to be maintained for any m -point direct correlation function $C^{(m)}$ and its Fourier transform $\hat{C}^{(m)}(\mathbf{q}_1, \mathbf{q}_2, \dots, \mathbf{q}_{m-1})$. If expanding $\hat{C}^{(m)}$ as a power series of wave vector \mathbf{q}_i , the resulting terms are of the form $\prod_{i=1}^{m-1} \prod_{\alpha=x,y,z} q_{i\alpha}^{n_{i\alpha}}$ ($n_{i\alpha} = 0, 1, 2, \dots$), the majority of which are, however, not rotationally invariant. Alternatively, this expansion can be expressed in an equivalent form, $\hat{C}^{(m)}(\mathbf{q}_1, \mathbf{q}_2, \dots, \mathbf{q}_{m-1}) = \sum_{K=0}^{\infty} \sum_{i_1, \dots, i_{m-1}} \sum_{\alpha_1, \dots, \alpha_{m-1}} C_{i_1 \alpha_1 \dots i_{m-1} \alpha_{m-1}} T_{i_1 \alpha_1 \dots i_{m-1} \alpha_{m-1}}^{(K)}$, where $T_{i_1 \alpha_1 \dots i_{m-1} \alpha_{m-1}}^{(K)} = q_{i_1 \alpha_1} \cdots q_{i_{m-1} \alpha_{m-1}}$ can be viewed as components of a tensor $\mathbf{T}^{(K)}$ of rank K . Thus the rotational invariance condition of this expansion would be satisfied if these tensor components are invariant under a proper orthogonal group $O^+(2)$ or $O^+(3)$ transformation (i.e., 2D or 3D rotation), which is the definition of an isotropic Cartesian tensor. Given the property of isotropic tensors which can be written as linear combinations of the products of Kronecker deltas $\delta_{\alpha_i \alpha_j}$ (for even rank K) or their product with only one Levi-Civita permutation tensor $\epsilon_{\alpha_k \alpha_l \alpha_p}$ (for odd K , with $\alpha_k, \alpha_l, \alpha_p = x, y, z$) in 2D or 3D Euclidean space [34–36], the corresponding rotationally invariant form of $\hat{C}^{(m)}$ expansion can be expressed in terms of $\mathbf{q}_i \cdot \mathbf{q}_j$ and $(\mathbf{q}_k \times \mathbf{q}_l) \cdot \mathbf{q}_p$, i.e.,

$$\begin{aligned} \hat{C}^{(m)}(\mathbf{q}_1, \mathbf{q}_2, \dots, \mathbf{q}_{m-1}) &= \sum_{\mu_1, \dots, \mu_{m-1}} \hat{C}_{\mu_1, \dots, \mu_{m-1}}^{(m)} \prod_{i,j=1}^{m-1} (\mathbf{q}_i \cdot \mathbf{q}_j)^{\mu_{ij}} + \sum_{k,l,p=1}^{m-1} \sum_{v_1, \dots, v_{m-1}} \hat{C}_{v_1, \dots, v_{m-1}}^{(m)} \\ &\times \prod_{i,j=1}^{m-1} (\mathbf{q}_i \cdot \mathbf{q}_j)^{v_{ij}} [(\mathbf{q}_k \times \mathbf{q}_l) \cdot \mathbf{q}_p], \end{aligned} \quad (2)$$

with coefficients $\hat{C}_{\mu_1, \dots, \mu_{m-1}}^{(m)}$ and $\hat{C}_{v_1, \dots, v_{m-1}}^{(m)}$. Note that this is a general form of expansion but not an irreducible one.

For a two-point correlation, from Eq. (2) with $m = 2$ the only available expansion form is $(\mathbf{q} \cdot \mathbf{q})^M = q^{2M}$, i.e., $\hat{C}^{(2)}(\mathbf{q}) = \hat{C}_0 + \sum_{M=1}^{\infty} \hat{C}_M q^{2M}$. Its contribution to the

free-energy functional is given by (after rescaling)

$$\Delta \mathcal{F}^{(2)} = \int d\mathbf{r} \left\{ -\frac{\epsilon}{2} n^2 + \frac{\lambda}{2} n \prod_{i=0}^{N-1} [(\nabla^2 + Q_i^2)^2 + b_i] n \right\}, \quad (3)$$

where ϵ , λ , Q_i , and b_i can be expressed via the expansion coefficients \hat{C}_M . This leads to the multimode PFC model presented in Ref. [10], with wave numbers Q_i determining N different length scales (bond lengths).

When $m = 3$, the general form of $\hat{C}^{(3)}(\mathbf{q}_1, \mathbf{q}_2)$ reads

$$\begin{aligned} \hat{C}^{(3)}(\mathbf{q}_1, \mathbf{q}_2) &= \hat{C}_0^{(3)} + \sum_{M=1}^{\infty} \left[\hat{C}_1^{(3)} q_1^{2M} + \hat{C}_2^{(3)} q_2^{2M} \right. \\ &+ \sum_{\mu=1}^{M-1} \hat{C}_{2\mu, 2M-2\mu}^{(3)} q_1^{2\mu} q_2^{2M-2\mu} \\ &+ \sum_{\mu=0}^{M-1} \sum_{\nu=0}^{M-1-\mu} \hat{C}_{2\mu, 2\nu, 2M-2\mu-2\nu}^{(3)} q_1^{2\mu} \\ &\left. \times q_2^{2\nu} (\mathbf{q}_1 \cdot \mathbf{q}_2)^{M-\mu-\nu} \right], \end{aligned} \quad (4)$$

with the corresponding free-energy contribution given by [see the Supplemental Material (SM) [37] for the derivation]

$$\begin{aligned} \Delta \mathcal{F}^{(3)} &= \int d\mathbf{r} \left\{ -\frac{1}{3} D_0 n^3 + \sum_{M=1}^{\infty} \left[D_M n^2 \nabla^{2M} n \right. \right. \\ &+ \sum_{\mu=1}^{M-1} D_{\mu, M-\mu} n (\nabla^{2\mu} n) (\nabla^{2M-2\mu} n) \\ &+ \sum_{\mu=1}^{M-1} \sum_{\nu=1}^{M-1-\mu} D_{\mu, \nu, M-\mu-\nu} (\nabla^{2\mu} n) \\ &\left. \left. \times (\nabla^{2\nu} n) (\nabla^{2M-2\mu-2\nu} n) \right] \right\}, \end{aligned} \quad (5)$$

where parameters D 's are dependent on the $\hat{C}^{(3)}$ coefficients. Interestingly, Eq. (5) shows that any terms of the $C^{(3)}$ free-energy contribution are always angle independent and isotropic (except for some special infinite series of $\hat{C}^{(3)}$ expansion [32,33]; see the SM [37]). This can be attributed to the fact that the cubic energy terms are governed by the resonant triads of reciprocal lattice vectors [10,38], i.e., $\mathbf{q}_j + \mathbf{q}_k + \mathbf{q}_l = \mathbf{0}$, and the side lengths of this vector triangle ($|\mathbf{q}_j|, |\mathbf{q}_k|, |\mathbf{q}_l|$, i.e., lattice length scales) uniquely determine all three angles between the wave vectors and hence the bond (neighboring) orientations.

Thus we need a four- or higher-order direct correlation to obtain the explicit angle dependence, given that angles of a wave-vector polygon or skew polygon of more than three sides (with resonant condition $\sum_{i=1}^m \mathbf{q}_i = \mathbf{0}$, $m \geq 4$) cannot be uniquely determined by the side lengths. For $\hat{C}^{(4)}$ all the free-energy terms are derived in the SM, including two types of isotropic terms, n^4 and $n(\nabla^{2\mu} n)(\nabla^{2\nu} n)(\nabla^{2M-2\mu-2\nu} n)$ (with integers $\mu, \nu \geq 0$, $M \geq \mu + \nu$), and three types of angle-

dependent terms,

$$\begin{aligned}
 f_{a1}^{(4)} &= [\nabla^{2\mu}(n\nabla^{2\omega}n)](\nabla^{2\nu}n)(\nabla^{2M-2\mu-2\nu-2\omega}n), \\
 f_{a2}^{(4)} &= \sum_{\alpha_i, \beta_j=x,y,z} \left[\nabla^{2\mu} \left(n \nabla^{2\omega} \prod_{i=1}^{\kappa} \prod_{j=1}^{\tau} \partial_{\alpha_i} \partial_{\beta_j} n \right) \right] \\
 &\quad \times \left(\nabla^{2\nu} \prod_{i=1}^{\kappa} \partial_{\alpha_i} n \right) \left(\nabla^{2M-2\mu-2\nu-2\omega-2\kappa-2\tau} \prod_{j=1}^{\tau} \partial_{\beta_j} n \right), \\
 f_{a3}^{(4)} &= n \sum_{\alpha_i, \beta_j, \gamma_k} \sum_{\alpha, \beta, \gamma} \epsilon_{\alpha\beta\gamma} \left(\nabla^{2\mu} \prod_{i=1}^{\kappa} \prod_{k=1}^{\lambda} \partial_{\alpha_i} \partial_{\gamma_k} \partial_{\alpha} n \right) \\
 &\quad \times \left(\nabla^{2\nu} \prod_{i=1}^{\kappa} \prod_{j=1}^{\tau} \partial_{\alpha_i} \partial_{\beta_j} \partial_{\beta} n \right) \left(\nabla^{2\omega} \prod_{j=1}^{\tau} \prod_{k=1}^{\lambda} \partial_{\beta_j} \partial_{\gamma_k} \partial_{\gamma} n \right),
 \end{aligned}$$

where $\alpha_i, \beta_j, \gamma_k, \alpha, \beta, \gamma = x, y, z$. For the example of $f_{a1}^{(4)}$ terms (with integers $\mu \geq 1, \nu, \omega \geq 0$ and $M \geq \mu + \nu + \omega$), if expanding the density field as $n = n_0 + \sum_j A_j \exp(i\mathbf{q}_j \cdot \mathbf{r})$, with the average density n_0 and amplitudes $A_j(\mathbf{q}_j) = A_{-j}^*(-\mathbf{q}_j)$, given a system of volume V , we have

$$\begin{aligned}
 &\frac{1}{V} \int d\mathbf{r} f_{a1}^{(4)} \Big|_{n_0=0} \\
 &= (-1)^M \sum_{ijkl} |\mathbf{q}_i + \mathbf{q}_j|^{2\mu} q_j^{2\omega} q_k^{2\nu} q_l^{2M-2\mu-2\nu-2\omega} \\
 &\quad \times A_i A_j A_k A_l \delta_{\mathbf{q}_i + \mathbf{q}_j + \mathbf{q}_k + \mathbf{q}_l, 0}. \quad (6)
 \end{aligned}$$

The resonant condition $\mathbf{q}_i + \mathbf{q}_j + \mathbf{q}_k + \mathbf{q}_l = \mathbf{0}$ is satisfied by three types of wave-vector combinations [10,39]: collinear ($\mathbf{q}_i - \mathbf{q}_i + \mathbf{q}_j - \mathbf{q}_j = \mathbf{0}$), pairwise ($\mathbf{q}_i - \mathbf{q}_i + \mathbf{q}_j - \mathbf{q}_j = \mathbf{0}$), and nonpairwise closed loops. For Eq. (6), the collinear contribution f^C from n_q wave vectors yields $f^C = (-1)^M 2^{2\mu+1} \sum_{j=1}^{n_q} q_j^{2M} |A_j|^4$, while the angle dependence arises from the factor $|\mathbf{q}_i + \mathbf{q}_j|^{2\mu}$ if $\mu \geq 2$ for pairwise resonant tetrads and $\mu \geq 1$ for nonpairwise ones.

For some crystalline structures (e.g., five 2D Bravais lattices and some 3D ones) the pairwise contributions would be sufficient in determining the phase stability. Given any pair $(\mathbf{q}_i, \mathbf{q}_j)$ with angle θ and $q_j = \gamma q_i \equiv \gamma q$ ($i \neq j$), the pairwise (P) contribution of Eq. (6) gives

$$\begin{aligned}
 &\frac{1}{V} \int d\mathbf{r} [\nabla^{2\mu}(n\nabla^{2\omega}n)](\nabla^{2\nu}n)(\nabla^{2M-2\mu-2\nu-2\omega}n) \Big|_{n_0=0}^{(P)} \\
 &= 2(-1)^M [(1 + \gamma^2 + 2\gamma \cos \theta)^\mu + (1 + \gamma^2 - 2\gamma \cos \theta)^\mu] \\
 &\quad \times q^{2M} (\gamma^{2M-2\mu-2\nu-2\omega} + \gamma^{2\nu}) (1 + \gamma^{2\omega}) |A_i|^2 |A_j|^2, \quad (7)
 \end{aligned}$$

the minimization of which leads to $\cos \theta = 0$ when $(-1)^M > 0$. A similar outcome is obtained for all other angle-dependent $\hat{C}^{(4)}$ contributions [37], indicating that a single quartic gradient term would favor only the $\pi/2$ orientation when considering pairwise wave vectors.

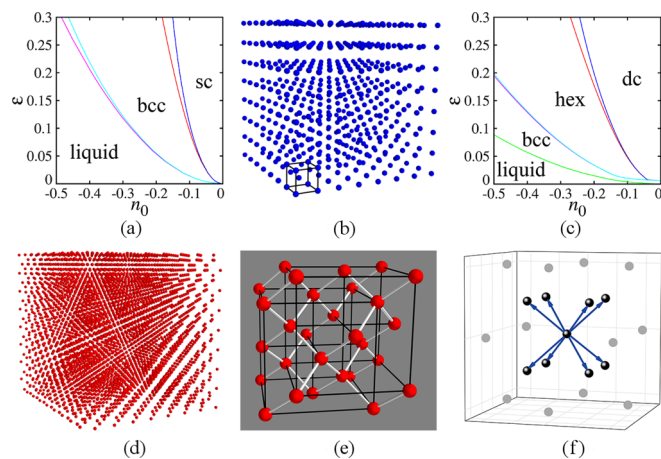


FIG. 1. Phase diagrams determined by Eq. (8) at $\lambda = 1$ and $(E_0, E_{11}, E_{44}) = (1, 25/72, 1/16)$ for (a) and $(1/18, 0, 1/32)$ for (c). Sample sc (b) and dc (d) structures are obtained from simulations with a 64^3 grid size, for $n_0 = -0.01$ and $\epsilon = 0.02$. An enlarged portion of (d) is shown in (e), while (f) gives the diffraction pattern of (d).

To verify this result we study a 3D example with only one length scale (i.e., one mode with $q_0 = 1$ and $\gamma = 1$),

$$\begin{aligned}
 \mathcal{F} &= \int d\mathbf{r} \left[-\frac{1}{2} \epsilon n^2 + \frac{1}{2} \lambda n (\nabla^2 + q_0^2)^2 n + \frac{1}{4} E_0 n^4 \right. \\
 &\quad \left. + E_{11} n^3 \nabla^2 n + E_{44} n^2 \nabla^4 n^2 \right], \quad (8)
 \end{aligned}$$

where the only angle-dependent term is $n^2 \nabla^4 n^2$ (i.e., $M = \mu = 2$ and $\nu = \omega = 0$, reproducing that used previously in 2D square pattern formations [30,31]). From the above analysis, the simple cubic (sc) phase, characterized by a bond angle $\theta = \pi/2$ and basic wave vectors $(1, 0, 0)$, $(0, 1, 0)$, $(0, 0, 1)$, should be stabilized for n_0 close to 0. This is consistent with our numerical result in Fig. 1(b), for which the simulation starts from a homogeneous state with random initial condition and follows the dynamics $\partial n / \partial t = \nabla^2 \delta \mathcal{F} / \delta n$. The phase diagram is given in Fig. 1(a), as calculated via a one-mode approximation.

To model structures characterized by other angles, the parameters need to be chosen such that the contributions from nonpairwise wave vectors would be important. For the example of a diamond cubic (dc) phase, in the first mode with amplitude A , $\mathbf{q}_1 = q_0(-1, 1, 1)/\sqrt{3}$, $\mathbf{q}_2 = q_0(1, -1, 1)/\sqrt{3}$, $\mathbf{q}_3 = q_0(1, 1, -1)/\sqrt{3}$, and $\mathbf{q}_4 = q_0(-1, -1, -1)/\sqrt{3}$, thus $\mathbf{q}_1 + \mathbf{q}_2 + \mathbf{q}_3 + \mathbf{q}_4 = \mathbf{0}$, yielding $\cos \theta = -1/3$ and $\theta = 109.47^\circ$. The corresponding nonpairwise contribution of Eq. (6) is then given by $(-1)^{M+1} 48 q_0^{2M} 2^\mu (1 + \cos \theta)^\mu |A|^4$. Combining with Eq. (7), we can identify the parameters minimizing \mathcal{F} of Eq. (8) that favor the dc structure, with results (including the phase diagram and a simulated structure emerging from initial homogeneous state) shown in Figs. 1(c)–1(f). Note that due to the incorporation of angle dependence, only one mode is needed to generate a sc or dc phase, different from previous isotropic PFC models where three [8] or two [24] modes are required.

An important feature of this approach is the ability to continuously control the characteristic angles of the crystalline phases, as achieved by combining angle-dependent gradient terms, e.g., $\sum_k E_k n (\nabla^{2\mu_k} n^2) (\nabla^{2M_k - 2\mu_k} n)$, so that the angle

can be tuned via coefficients E_k . For the case of a single adjustable angle θ between any pair of wave vectors ($\mathbf{q}_i, \mathbf{q}_j$), the simplest combination is $E_1 n(\nabla^{2\mu_1} n^2)(\nabla^{2M_1-2\mu_1} n) + E_2 n(\nabla^{2\mu_2} n^2)(\nabla^{2M_2-2\mu_2} n)$. For the structures dominated by pairwise and collinear wave vector contributions, Eq. (7) gives

$$f^P = \frac{1}{V} \int d\mathbf{r} \sum_{k=1}^2 E_k n(\nabla^{2\mu_k} n^2)(\nabla^{2M_k-2\mu_k} n) \Big|_{n_0=0}^{(P)}$$

$$= 4\{E_1[(1 + \gamma^2 + 2\gamma \cos \theta)^{\mu_1} + (1 + \gamma^2 - 2\gamma \cos \theta)^{\mu_1}] \times (-1)^{M_1} q^{2M_1} (1 + \gamma^{2M_1-2\mu_1}) + E_2[(1 + \gamma^2 + 2\gamma \cos \theta)^{\mu_2} + (1 + \gamma^2 - 2\gamma \cos \theta)^{\mu_2}] \times (-1)^{M_2} q^{2M_2} (1 + \gamma^{2M_2-2\mu_2})\} |A_i|^2 |A_j|^2, \quad (9)$$

while the collinear contribution is angle independent, i.e., $f^C = \sum_{k=1}^2 (-1)^{M_k} q^{2M_k} 2^{2\mu_k+1} E_k (|A_i|^4 + \gamma^{2M_k} |A_j|^4)$. By minimizing f^P we get $\sin \theta = 0$ or

$$-\frac{E'_2}{E'_1} [(1 + \gamma^2 + 2\gamma \cos \theta)^{\mu_2-1} - (1 + \gamma^2 - 2\gamma \cos \theta)^{\mu_2-1}] = (1 + \gamma^2 + 2\gamma \cos \theta)^{\mu_1-1} - (1 + \gamma^2 - 2\gamma \cos \theta)^{\mu_1-1}, \quad (10)$$

where $E'_k = (-1)^{M_k} q^{2M_k} \mu_k E_k (1 + \gamma^{2M_k-2\mu_k})$ ($k = 1, 2$). It is straightforward to show that the lowest-order terms giving adjustable values of nonzero θ for f^P minimization are of $\mu_1 = 4$ and $\mu_2 = 2$, when $(-1)^{M_1} E_1 > 0$ and $(-1)^{M_2} E_2 < 0$, thus $\cos^2 \theta = -[E'_2/E'_1 + 3(1 + \gamma^2)^2]/4\gamma^2$ from Eq. (10). To ensure the results are independent of wave number q , we set $M_1 = M_2 = M$ and to lowest order $M = \mu_1 = 4, \mu_2 = 2$, leading to the combination $E_1 n^2 \nabla^8 n^2 + E_2 n(\nabla^4 n^2)(\nabla^4 n)$ and

$$\frac{E_2}{E_1} = -\frac{4}{1 + \gamma^4} [3(1 + \gamma^2)^2 + 4\gamma^2 \cos^2 \theta], \quad E_1 > 0, \quad (11)$$

i.e., at least eighth-order gradient terms are needed to obtain the angle control in structures governed by pairwise resonant wave vectors. The free-energy functional is then

$$\mathcal{F} = \int d\mathbf{r} \left[-\frac{\epsilon}{2} n^2 + \frac{\lambda}{2} n \prod_{i=0}^{N-1} (\nabla^2 + Q_i^2)^2 n + E_1 n^2 \nabla^8 n^2 + E_2 n(\nabla^4 n^2)(\nabla^4 n) + E_3 (\nabla^2 n^2)(\nabla^4 n)(\nabla^2 n) + \frac{E_0}{4} n^4 \right], \quad (12)$$

where the E_3 term is angle independent for pairwise wave vectors and is introduced for structure stability.

We first apply the above analysis to the modeling of 2D rhombic and square phases with continuous angle selection ($0 < \theta \leq \pi/2$), using one mode with $N = Q_0 = \gamma = 1$ and the basic wave vectors $\mathbf{q}_{1,2} = [\mp \cos(\theta/2), \sin(\theta/2)]$. Some simulation results are illustrated in Fig. 2, for five sample rhombic structures with $\theta = 30^\circ, 45^\circ, 55^\circ, 70^\circ, 85^\circ$, starting from a homogeneous initial state. The parameter ratio E_2/E_1 is chosen according to Eq. (11), and $E_3 = 0$. The resulting structures with desired angles are corroborated by the associated

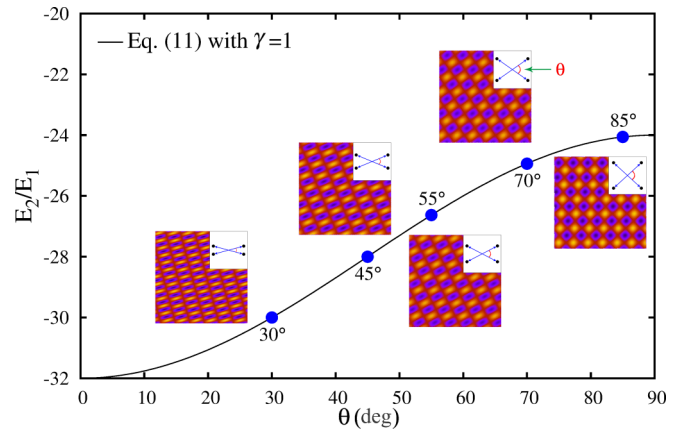


FIG. 2. Angle control for the rhombic phase, based on the prediction of Eq. (11) for E_2/E_1 vs θ (solid curve). Simulated structures and diffraction patterns are obtained with $n_0 = 0$, $\epsilon = 0.01$, $E_0 = 1/3$, $E_3 = 0$, and $(\lambda, E_1) = (600, 1/750)$ for $\theta = 85^\circ$ and 70° , $(2 \times 10^4, 1/750)$ for $\theta = 55^\circ$, $(6 \times 10^4, 1/800)$ for $\theta = 45^\circ$, and $(6 \times 10^5, 1.104 \times 10^{-3})$ for $\theta = 30^\circ$.

diffraction patterns (Fig. 2 insets), indicating the capability of angle control via nonlinear gradient terms.

Similar outcomes of continuous angle control can be obtained in 3D from Eqs. (11) and (12), with an example of simple monoclinic phase presented in Fig. 3. Three modes, $Q_0 : Q_1 : Q_2 = 1 : \gamma_2 : \gamma_3$, are needed here, with basic wave vectors $\mathbf{q}_1 = (1, 0, 0)$, $\mathbf{q}_2 = (0, \gamma_2, 0)$, and $\mathbf{q}_3 = (\gamma \cos \theta, 0, \gamma \sin \theta)$ with $\gamma \equiv \gamma_3$. This gives $\theta_{12} = \theta_{23} = \pi/2$, where θ_{ij} is the angle between \mathbf{q}_i and \mathbf{q}_j , and $\theta_{13} \equiv \theta$ is the only tunable angle determined by Eq. (11). The corresponding structures of different θ , including simple orthorhombic with $\theta = \pi/2$, have been obtained in our numerical simulations using random initial and periodic boundary conditions (Fig. 3). Note that this modeling procedure is also applicable to other angle-adjustable

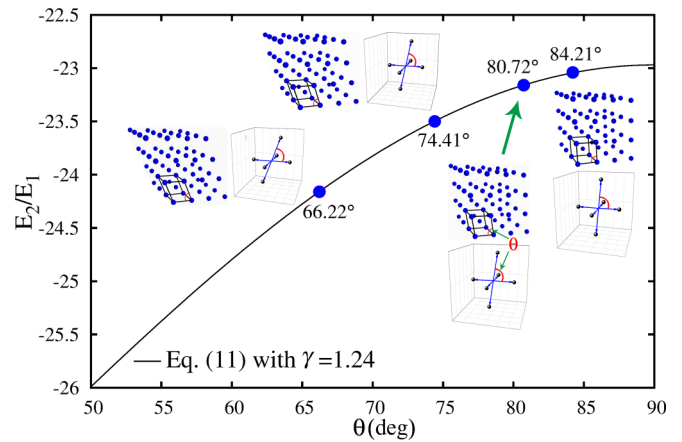


FIG. 3. Angle control for simple monoclinic structures with $Q_0 : Q_1 : Q_2 = 1 : 1.16 : 1.24$, based on the prediction of Eq. (11). A portion of the simulated system and the diffraction pattern are shown for each angle, with $n_0 = 0$, $\epsilon = 0.01$, $E_0 = 1/2$, $E_1 = 1/240$, $E_3 = 5/32$, and $\lambda = 5 \times 10^6$ for $\theta = 66.22^\circ$ and 5×10^5 for $\theta = 74.41^\circ, 80.72^\circ, 84.21^\circ$.

phases, such as rhombohedral (trigonal) or a more complex case of triclinic (with three modes and three tunable angles). All these results thus verify the effect of angle tuning and control on the emergence of crystalline phases through contributions of quartic coupling.

It is also important to note that although the model introduced above involves high-order nonlinear gradient terms, the related computational cost is modest when using the pseudospectral numerical algorithm, particularly for the cases of weak segregation (i.e., small ϵ) simulated here. In addition, such a format with spatial gradient terms has the advantage of being more feasible for the construction of amplitude equation formalism describing slowly varying mesoscopic scales [13,14,18,22], which is important for large-scale simulations with high computational efficiency and is the subject of our future research.

In summary, we have constructed a complete density field formulation integrating the microscopic property of interparticle bond-angle anisotropy and the requirement of global-scale system rotational invariance. Our results demonstrate that effects of angle dependency and adjustment are incorporated explicitly through quartic correlation in the system,

but not through any finite-order cubic coupling which instead implicitly affects angle selection via lattice length scales. The resulting nonlinear gradient terms of the atomic density field have been utilized to model various crystalline phases and, importantly, their bond-angle control. Since the model developed here already incorporates system elasticity and plasticity as in other PFC-type models, it can be readily applied to the study or prediction of a broad range of crystalline or polycrystalline material systems and more complex phases with bond anisotropy, their elastoplastic and defect properties, and nonequilibrium phenomena during crystallization and growth. This approach is built on the full-order expansion of direct correlation functions and the application of isotropic Cartesian tensors, and is thus of a generic nature and applicable to different types of ordering or self-assembling systems with varying atomistic details.

Z.-F.H. acknowledges support from the National Science Foundation under Grant No. DMR-1609625. Z.R.L. was supported by the National Natural Science Foundation of China under Grant No. 21773002.

-
- [1] K. R. Elder, M. Katakowski, M. Haataja, and M. Grant, *Phys. Rev. Lett.* **88**, 245701 (2002); K. R. Elder and M. Grant, *Phys. Rev. E* **70**, 051605 (2004).
- [2] K. R. Elder, N. Provatas, J. Berry, P. Stefanovic, and M. Grant, *Phys. Rev. B* **75**, 064107 (2007).
- [3] J. Li, S. Sarkar, W. T. Cox, T. J. Lenosky, E. Bitzek, and Y. Z. Wang, *Phys. Rev. B* **84**, 054103 (2011).
- [4] Y. M. Jin and A. G. Khachatryan, *J. Appl. Phys.* **100**, 013519 (2006).
- [5] Y. Singh, *Phys. Rep.* **207**, 351 (1991).
- [6] H. Löwen, *Phys. Rep.* **237**, 249 (1994).
- [7] S. van Teeffelen, R. Backofen, A. Voigt, and H. Löwen, *Phys. Rev. E* **79**, 051404 (2009).
- [8] M. Greenwood, N. Provatas, and J. Rottler, *Phys. Rev. Lett.* **105**, 045702 (2010).
- [9] K.-A. Wu, A. Adland, and A. Karma, *Phys. Rev. E* **81**, 061601 (2010).
- [10] S. K. Mkhonta, K. R. Elder, and Z.-F. Huang, *Phys. Rev. Lett.* **111**, 035501 (2013); **116**, 205502 (2016).
- [11] E. J. Schwalbach, J. A. Warren, K.-A. Wu, and P. W. Voorhees, *Phys. Rev. E* **88**, 023306 (2013).
- [12] G. Kocher and N. Provatas, *Phys. Rev. Lett.* **114**, 155501 (2015).
- [13] Z.-F. Huang, K. R. Elder, and N. Provatas, *Phys. Rev. E* **82**, 021605 (2010).
- [14] R. Spatschek and A. Karma, *Phys. Rev. B* **81**, 214201 (2010).
- [15] H. Emmerich, H. Löwen, R. Wittkowski, T. Gruhn, G. I. Tóth, G. Tegze, and L. Gránásy, *Adv. Phys.* **61**, 665 (2012).
- [16] P. Y. Chan, G. Tsekis, J. Dantzig, K. A. Dahmen, and N. Goldenfeld, *Phys. Rev. Lett.* **105**, 015502 (2010).
- [17] G. I. Tóth, T. Pusztai, G. Tegze, G. Tóth, and L. Gránásy, *Phys. Rev. Lett.* **107**, 175702 (2011).
- [18] N. Ofori-Opoku, J. Stolle, Z.-F. Huang, and N. Provatas, *Phys. Rev. B* **88**, 104106 (2013).
- [19] R. Backofen, K. Barmak, K. R. Elder, and A. Voigt, *Acta Mater.* **64**, 72 (2014).
- [20] J. Berry, J. Rottler, C. W. Sinclair, and N. Provatas, *Phys. Rev. B* **92**, 134103 (2015).
- [21] P. Hirvonen, M. M. Ervasti, Z. Fan, M. Jalalvand, M. Seymour, S. M. Vaez Allaei, N. Provatas, A. Harju, K. R. Elder, and T. Ala-Nissila, *Phys. Rev. B* **94**, 035414 (2016).
- [22] Z.-F. Huang, *Phys. Rev. E* **93**, 022803 (2016); **87**, 012401 (2013).
- [23] D. Taha, S. K. Mkhonta, K. R. Elder, and Z.-F. Huang, *Phys. Rev. Lett.* **118**, 255501 (2017).
- [24] V. W. L. Chan, N. Pisutha-Armond, and K. Thornton, *Phys. Rev. E* **91**, 053305 (2015).
- [25] P. Subramanian, A. J. Archer, E. Knobloch, and A. M. Rucklidge, *Phys. Rev. Lett.* **117**, 075501 (2016).
- [26] E. Alster, K. R. Elder, J. J. Hoyt, and P. W. Voorhees, *Phys. Rev. E* **95**, 022105 (2017).
- [27] P. J. Steinhardt, D. R. Nelson, and M. Ronchetti, *Phys. Rev. B* **28**, 784 (1983).
- [28] M. V. Jarić, *Phys. Rev. Lett.* **55**, 607 (1985).
- [29] K.-A. Wu, M. Plapp, and P. W. Voorhees, *J. Phys.: Condens. Matter* **22**, 364102 (2010).
- [30] M. R. E. Proctor, *J. Fluid Mech.* **113**, 469 (1981); V. L. Gertsberg and G. I. Sivashinsky, *Prog. Theor. Phys.* **66**, 1219 (1981).
- [31] M. Bestehorn and C. Pérez-García, *Physica D* **61**, 67 (1992).
- [32] M. Seymour and N. Provatas, *Phys. Rev. B* **93**, 035447 (2016).
- [33] E. Alster, D. Montiel, K. Thornton, and P. W. Voorhees, *Phys. Rev. Mater.* **1**, 060801 (2017).
- [34] H. Jeffreys, *Proc. Cambridge Philos. Soc.* **73**, 173 (1973).
- [35] E. A. Kearsley and J. T. Fong, *J. Res. Natl. Bur. Stand., Sect. B* **79**, 49 (1975).
- [36] P. G. Appleby, B. R. Duffy, and R. W. Ogden, *Glasgow Math. J.* **29**, 185 (1987).

- [37] See Supplemental Material at <http://link.aps.org/supplemental/10.1103/PhysRevB.97.180102> for the derivation of the complete free-energy contributions from $\hat{C}^{(3)}$ and $\hat{C}^{(4)}$ expansions that are rotationally invariant, the angle dependence of $\hat{C}^{(4)}$ free-energy terms and conditions of angle control, and the angle dependency for $C^{(3)}$ infinite series expansions in Refs. [32,33].
- [38] S. Alexander and J. McTague, *Phys. Rev. Lett.* **41**, 702 (1978).
- [39] J. L. Jones and M. Olvera de la Cruz, *J. Chem. Phys.* **100**, 5272 (1994).